FAST AND HIGH-RESOLUTION 3-D IMAGING ALGORITHM WITH SPECTRUM SHIFT FOR UWB PULSE RADARS

Shouhei Kidera, Takuya Sakamoto and Toru Sato
Graduate School of Informatics, Kyoto University, Japan

Keywords: UWB pulse radars, high-resolution and fast 3-D imaging, envelope of spheres, spectrum offset correction

Abstract

UWB pulse radar systems are promising candidates for a high range resolution imaging in a near field. We have already proposed rapid and robust imaging algorithm with envelope of spheres. It can realize stable 3-D imaging for an arbitrary target shape without derivative operations. However, the estimated image with this method is distorted especially around the target edges and wedges due to waveform deformations. In this paper, we propose fast and high-resolution 3-D imaging algorithm by directly compensating for these distortions with a spectrum offset correction. The application examples with numerical simulations and an experiment verify that the proposed method accomplishes high-speed, accurate 3-D imaging, including target edges, with the order of 1/100 center wavelength of the UWB pulse.

1. Introduction

UWB pulse radar has a great advantage for a high range-resolution in the proximity imaging. It is required for the non-destructive measurement for specular and precision products, such as reflector antennas and bodies of aircraft. It is also applicable to the target positioning or the self-localization systems for robots or automobiles. While many imaging algorithms for radar systems have been proposed, they require an intensive computation, and have an insufficient accuracy for our assumed applications [1–4]. Contrarily, we have already proposed a fast 3-D imaging algorithm called SEABED with a reversible transform between the received signals and the target shape [5, 6]. The similar ideas have been developed for the geosurface measurement, and the surface extraction for the breast cancer detection [7, 8]. Although SEABED can realize a real-time application, the estimated image can be readily fluctuated with a random noise because it utilizes a derivative operation. We already proposed fast and robust 3-D imaging algorithm based on envelopes of spheres to enhance the robustness [9, 10]. While this method accomplishes stable 3-D imaging even in noisy situations, the accuracy of this method depends on the target shape, especially around the target edges and wedges. This is because the scattered waveform is deformed compared to the transmitted one, and it causes the error for time delays. To enhance the accuracy of the estimated image, we have proposed an accurate imaging method, which iterates the shape and fast waveform estimation, simultaneously [11, 12]. It is confirmed that this method enables us to realize an accurate imaging in real environment for the 2-D problem. However, it requires more than 10 sec for the calculation in the case of the 3-D problem, which must be resolved for the real time operation.

In this paper, we propose fast, robust and accurate 3-D imaging algorithm with the idea of spectrum offset correction to resolve the above difficulties. This method can realize a direct compensation for the range shift with the spectrum offset correction between the scattered and transmitted signals. Numerical simulations and an experimental results show that the proposed method achieves the accurate 3-D imaging, which is suitable for our assumed applications.

2. System model

The upper side of Fig. 1 shows the system model. It assumes that the target has a clear boundary, and that the propagation speed of the radio wave is a known constant. An omni-directional antenna is scanned on a plane as $z = 0$. We utilize a monocycle pulse as the transmitting current and, assume the linear polarization in the direction of x axis. R-space is defined as the real space where targets and the antenna are located, and is expressed with the parameter (x, y, z). These parameters of the coordinate are normalized by λ, which is the center wavelength of the pulse. We assume $z > 0$ for simplicity. $s'(X, Y, Z')$ is defined as the received electric field at the antenna location $(x, y, z) = (X, Y, 0)$, where $Z' = ct/(2\lambda)$ is expressed by the time t and the speed of the radio wave c. $s(X, Y, Z')$ is defined as the output of the filter. We connect the significant peaks of $s(X, Y, Z')$ as Z for each X and Y, and extract the surface (X, Y, Z), which is called a quasi wavefront. D-space is defined as the space expressed by (X, Y, Z). The transform from d-space to r-space corresponds to the imaging which we deal with in this paper.

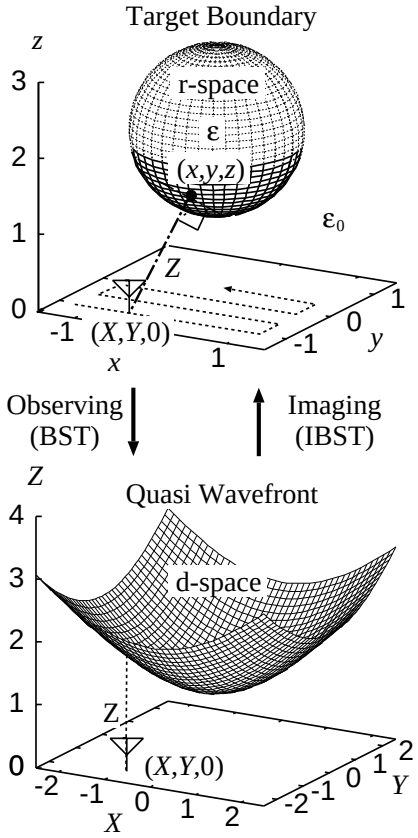

Fig. 1. Relationship between r-space (Upper) and d-space (Lower).

3. Conventional method

We have already proposed the rapid 3-D imaging algorithm as SEABED, which is based on the reversible transform BST (Boundary Scattering Transform) between the target boundary (x, y, z) and the quasi wavefront (X, Y, Z) [6]. Inverse BST is expressed as $x = X - Z\partial Z/\partial X,\ y = Y - Z\partial Z/\partial Y, z = Z\sqrt{1-(\partial Z/\partial X)^2-(\partial Z/\partial Y)^2}$. Fig. 1 shows the relationship between r-space and d-space. While this method realizes high-speed 3-D imaging, the estimated image is readily fluctuated with random noise because it utilizes the derivatives of the quasi wavefront. To enhance the robustness, we have developed rapid and robust 3-D imaging algorithm with the envelopes of the spheres as Envelope [9, 10]. This method is based on the principle that the target boundaries can be expressed as the envelope of the spheres, whose center is $(X, Y, 0)$ and radius Z. Fig. 2 shows the relationship between the target boundary and an envelope of the circles in 2-D problems, for simplicity. It achieves robust and fast 3-D imaging for an arbitrary target shape without derivative operations. In addition, this method enables us to compensate the phase rotation of scattered waves

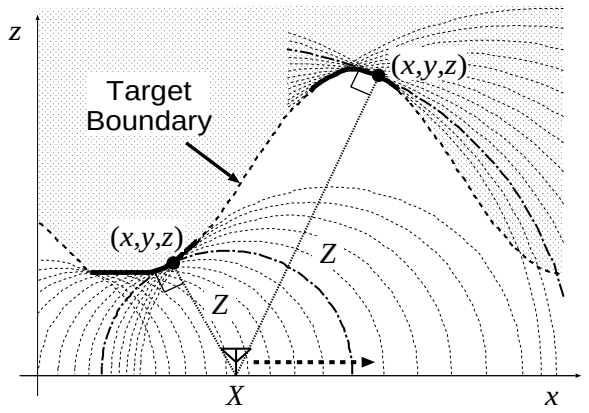

Fig. 2. Relationship between a target boundary and an envelope of circles.

due to passing through the caustic points. Thus, it also realizes an accurate 3-D imaging for the concave boundary.

However, the estimated image for the convex target is distorted around the target edges or wedges. Fig. 3 shows the estimated image with this method. Here, the dashed lines show the true shape. The image around the target edges is expressed as smoothed surface, and the edge points cannot be specified. This is because the scattered waveform from the edge region is significantly different from the transmitted one, and it causes a large error for the quasi wavefront. Fig. 4 shows the accuracy of the quasi wavefront for each antenna location. Here, $\epsilon = |Z_{\rm true} - Z|$. The errors around edge regions are over $7.0 \times 10^{-2}\lambda/\mathrm{c}$.

We have proposed an accurate imaging algorithm by synthesizing the shape and waveform estimations to enhance the resolution around the edge region, which is termed Envelope with WE (Envelope method with Waveform Estimation) [11, 12]. This method updates matched filters with the estimated waveform in each step, which can be calculated with the previously extracted target boundary. Each scattered waveform is calculated with the simplified Green's function integral along the path, which dominantly contributes to the scattering. By re-extracting the quasi wavefront with the updated matched filter, the target boundary is recursively calculated until the convergence condition is satisfied.

Figs. 5 and 6 show the estimated image and the accuracy for the quasi wavefront, respectively, where we iterate the shape and waveform estimation for 2 times. We confirm that the resolution and accuracy for the edge region are still insufficient, and the estimated image hardly converges to the true shape, even if we increase the number of the iteration. The errors around the edge region is more

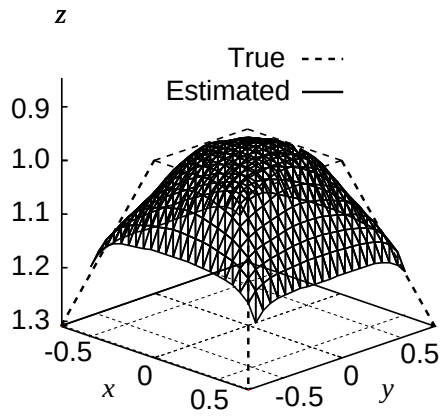

Fig. 3. Estimated image with Envelope.

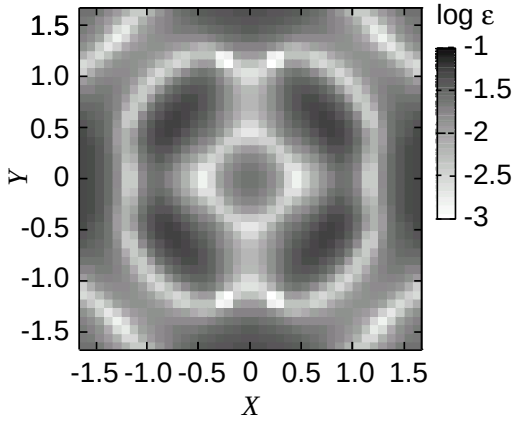

Fig. 4. Accuracy for quasi wavefront with Envelope.

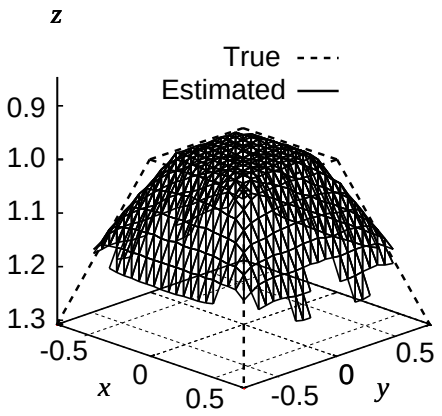

Fig. 5. Estimated image with Envelope with WE.

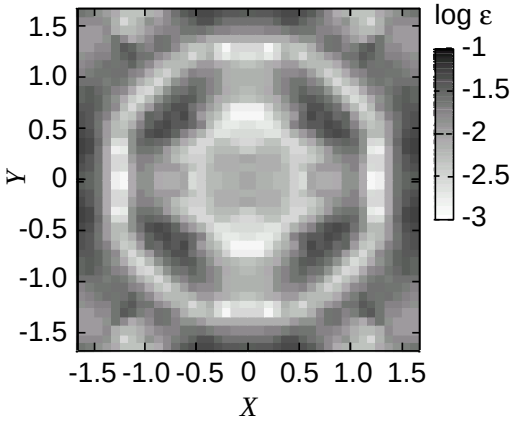

Fig. 6. Accuracy for the quasi wavefront with Envelope with WE.

than $3.0 \times 10^{-2}\lambda/\mathrm{c}$. The reason for these errors is that the accuracy for the waveform estimation is distorted, where the scattered wave includes a negligible influences from the shadow region of the target. Moreover, the calculation time of this method is more than 10 sec, which is not realistic to deal with the practical applications.

4. Proposed method

To resolve those problems, described in the previous section, we propose high-speed and accurate 3-D imaging with the spectrum offset correction. This method directly compensates for a range error of Z with the center frequencies of the waveforms. We confirm that the matching point between the scattered and transmitted signals does not express the true time of arrival due to the waveform deformations. Fig. 7 shows a matching example between the transmitted and scattered waveforms. The proposed method approximates the range shift ΔZ as

$$\Delta Z = \frac{f_o}{W}(f_{\mathrm{tr}}^{-1} - f_{\mathrm{sc}}^{-1}), \tag{1}$$

where f_{tr} and f_{sc} are the center frequencies of the transmitted and scattered waveforms, respectively. $f_0 = \mathrm{c}/\lambda$. W is a normalized constant, which is determined with a fractional bandwidth of the transmitted signal. $W = 4$ is set. f_{sc} is calculated in the time domain as [13],

$$f_{\mathrm{sc}} = \frac{1}{2\pi}\angle\left(\sum_{i=0}^{N} s_i^* \; s_{i+1}\right), \tag{2}$$

where $s_i = s\left(i\Delta t + 2Z\lambda/\mathrm{c}\right)$, $s(t)$ is an analytical signal of the scattered wave, Δt is the interval of the time sampling, and N is the total number of the samples. Eq. (2) enables us to calculate f_{sc} with eliminating the interferences from the multiple scattered or the direct waves because these components can be windowed in the time domain. Here, N is set to 100, where $\Delta t = 0.005\lambda/c$. The procedures of this method are summarized as follows. f_{tr} is given.

1. Extract the quasi wavefront as (X, Y, Z) by connecting the significant peaks of $s(X, Y, Z')$.
2. Calculate f_{sc} in Eq. (2) for each antenna location, and estimate the range shift ΔZ in Eq. (1).

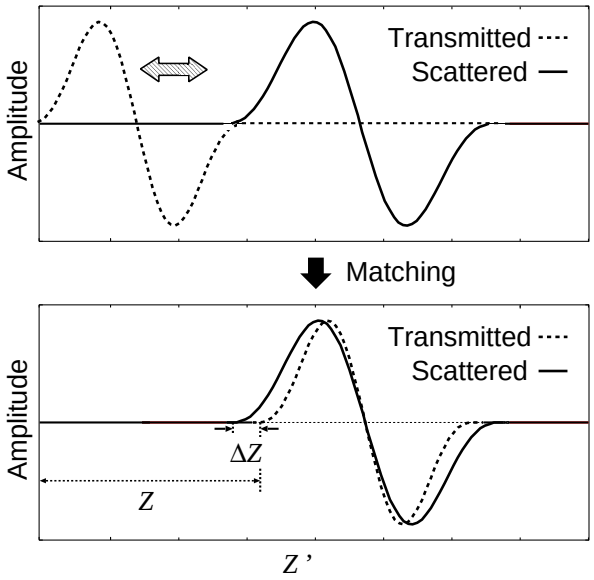

Fig. 7. Matching examples between scattered and transmitted waveforms.

3. Calculate z for each (x, y) as

$$z = \max_{X,Y \in \Gamma} \sqrt{(Z + \Delta Z)^2 - (x - X)^2 - (y - Y)^2}. \quad (3)$$

4. Remove the points on the spheres, which are calculated with the peripheral points of the quasi wavefront.

We call this method as Envelope with SOC (Envelope method with Spectrum Offset Correction). This method accomplishes rapid and high-resolution 3-D imaging with direct compensations for the quasi wavefronts.

5. Performance evaluation

5.1 Application example with numerical simulations

Figs. 8 and 9 show the estimated image, and the accuracy for the quasi wavefront with Envelope with SOC, respectively. We confirm that our method accomplishes more accurate imaging including the target edges and wedges. The error around this region is 0.01λ, and the calculation time of this method is 0.2 sec for Xeon 3.2 GHz processor, which can be applicable for the realtime operation. This is because the accuracy of the estimated image depends only on that of the quasi wavefront, which can be directly compensated without reconstructing the scattered waveform completely.

In addition, we confirm that it can realize an accurate 3-D imaging even in the noisy environment, for S/N $\geq$ 25 dB. These results verify that the proposed method accomplishes the high-performance imaging, in terms of speed, stability, and accuracy, which has never been obtained with the conventional works. The reason of this superiority is that this method specifies to extract the clear boundary with the correctly estimated time delays.

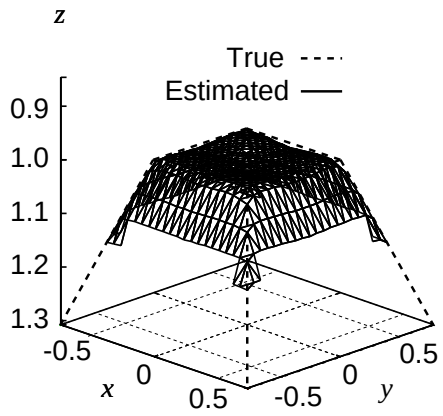

Fig. 8. Estimated image with Envelope with SOC.

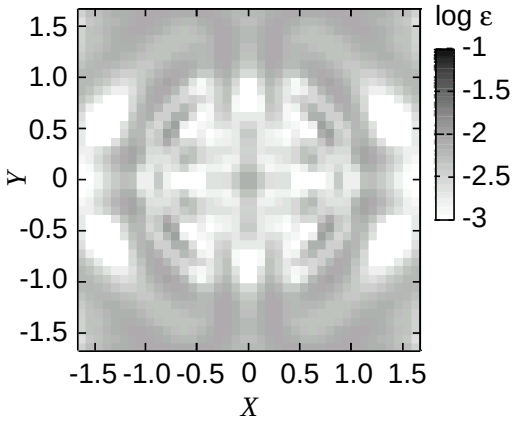

Fig. 9. Accuracy for the quasi wavefront with Envelope with SOC.

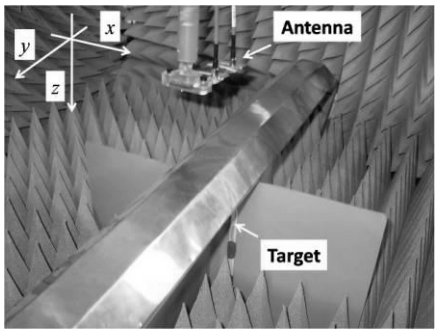

Fig. 10. Arrangement of the experiment.

5.2 Application example with experiment

This section describes the performance evaluation with the experiment. We utilize the UWB pulse with the center frequency of 3.3 GHz and the 10dB-bandwidth of 2.0 GHz. The antenna has an elliptic polarization whose ratio of the major to the minor

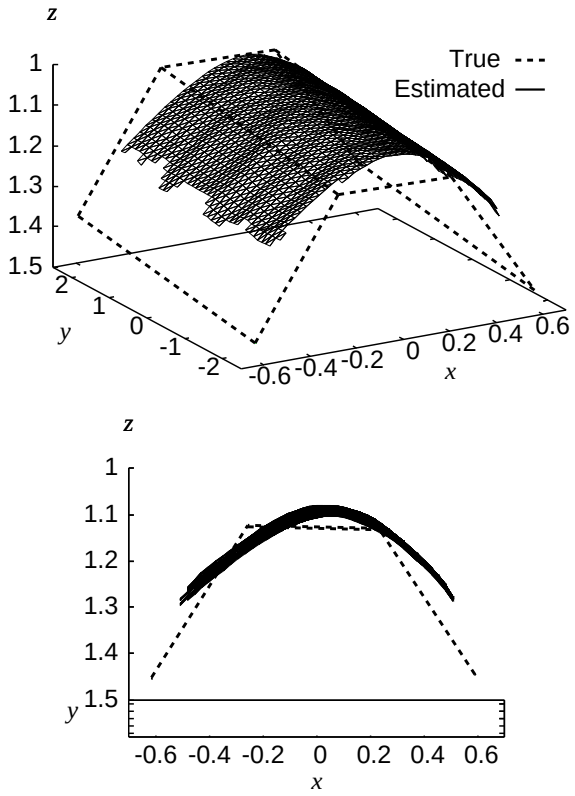

Fig. 11. Estimated image with Envelope in the experiment.

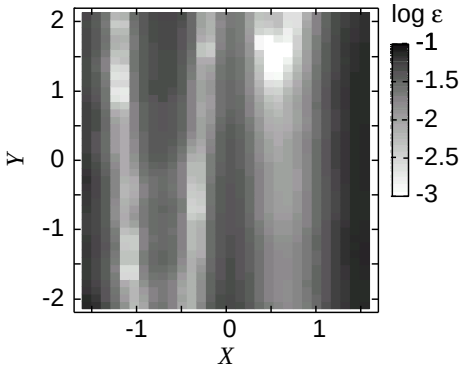

Fig. 12. Accuracy for the quasi wavefront with Envelope in the experiment.

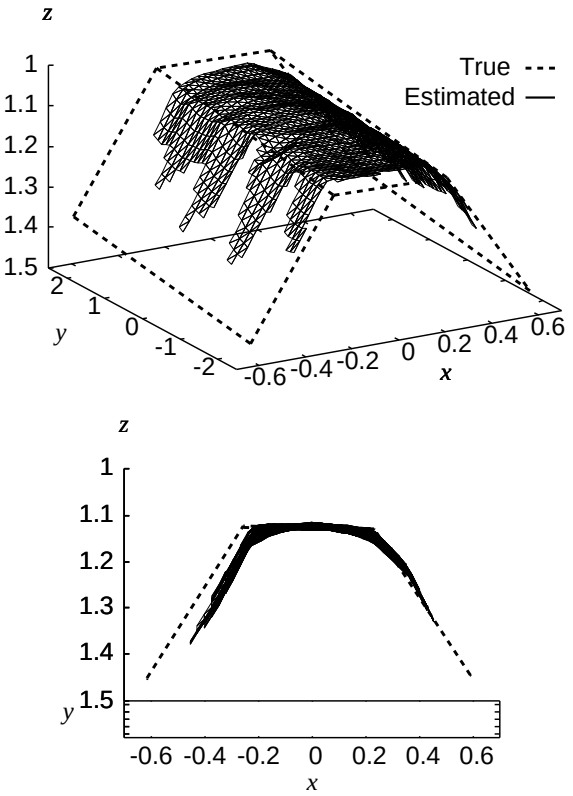

Fig. 13. Estimated image with Envelope with SOC in the experiment.

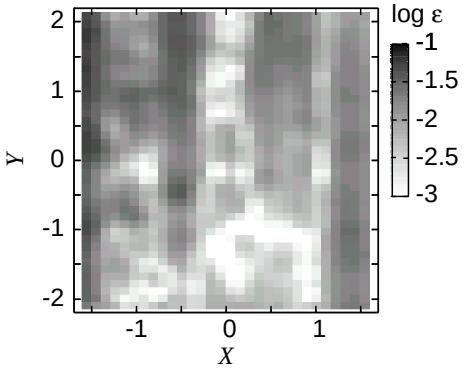

Fig. 14. Accuracy for the quasi wavefront with Envelope with SOC in the experiment.

axis is about 17 dB, and the direction of the polarimetry axis of the antenna is along the y axis. The 3dB-beamwidth of the antenna is about 90°. We set the trapezoid target, which is made of stainless steel sheet. Fig. 10 illustrates the location of the antenna and the target. The transmitted and received antennas are scanned on $z = 0$ plane, for -170 mm $\leq x \leq 170$ mm and -200 mm $\leq y \leq 200$ mm, respectively, where each sampling interval is set to 10 mm. The separation between the transmitted and received antennas is 48 mm in y-direction. The data are coherently averaged 1024 times.

Figs. 11 and 12 show the estimated image and the accuracy for the quasi wavefront with Envelope, respectively. S/N is 35dB. As shown in these figures, the accuracy for the target wedge is distorted around wedges due to the scattered waveform deformations. We quantitatively evaluate the accuracy of the image with an evaluation value μ that is defined as

$$\mu = \sqrt{\frac{1}{N_{\mathrm{T}}} \sum_{i=0}^{N_{\mathrm{T}}} \min_{\boldsymbol{x}} \|\boldsymbol{x} - \boldsymbol{x}_{\mathbf{e}}^{i}\|^2}, \tag{4}$$

where $\boldsymbol{x}$ and $\boldsymbol{x}_{\mathrm{e}}^{i}$ express the location of the true target point and that of the estimated point, respectively. N_{T} is the total number of the estimated points. μ with Envelope is $3.178 \times 10^{-2}\lambda$. Contrarily, Figs. 13 and 14 show the estimated image and the accuracy for the quasi wavefront with Envelope with SOC, respectively. These figures verify that the estimated image can be more accurately reconstructed around the wedges and the upper surface of the target. μ is $1.631 \times 10^{-2}\lambda$. However, there are some distortions in the estimated image, compared to the results in the numerical simulations. This is because the fractional bandwidth of the experimental pulse is lower than that of the mono-cycle pulse. Thus, the scattered wave is severely interfered with the remains of direct wave, which cannot be completely eliminated.

6. Conclusion

We proposed the 3-D imaging algorithm with the spectrum offset correction as Envelope+SOC. It realizes rapid and accurate 3-D imaging with the direct compensations for the quasi wavefront. The results in numerical simulations showed that the accuracy for the estimated image is 0.01λ, for S/N $\geq$ 25 dB, and the calculation time is 0.2 sec with Xeon 3.2 GHz processor. Moreover, we showed the application examples with with the experimental data. These investigations verified that our proposed method accomplishes more accurate imaging, even in real environment.

Acknowledgement

We thank Dr. Satoru Kurokawa at Advanced Industrial Science and Technology, Japan, and Mr. Satoshi Sugino at National Institute of the New Product Technologies Development Department, Matsushita Electric Works, Ltd, Japan for their valuable advices. This work is supported in part by the 21st Century COE Program (Grant No. 14213201).

References

[1] C. Chiu, C. Li, and W. Chan, "Image reconstruction of a buried conductor by the genetic algorithm," *IEICE Trans. Electron.*, vol. E84-C, no. 12, pp. 1946–1951, 2001.

[2] T. Takenaka, H. Jia, and T. Tanaka, "Microwave imaging of an anisotropic cylindrical object by a forward-backward time-stepping method," *IEICE Trans. Electron.*, vol. E84-C, no. pp. 1910–1916, 2001.

[3] T. Sato, K. Takeda, T. Nagamatsu, T. Wakayama, I. Kimura and T. Shinbo, "Automatic signal processing of front monitor radar for tunneling machines," *IEEE Trans. Geosci. Remote Sens.*, vol.35, no.2, pp.354-359, 1997.

[4] T. Sato, T. Wakayama, and K. Takemura, "An imaging algorithm of objects embedded in a lossy dispersive medium for subsurface radar data processing," *IEEE Trans. Geosci. Remote Sens.*, vol.38, no.1, pp.296–303, 2000.

[5] T. Sakamoto and T. Sato, "A target shape estimation algorithm for pulse radar systems based on boundary scattering transform," *IEICE Trans. Commun.*, vol.E87-B, no.5, pp. 1357–1365, 2004.

[6] T. Sakamoto, "A fast algorithm for 3-dimensional imaging with UWB pulse radar systems," *IEICE Trans. Commun.*, vol.E90-B, no.3, pp. 636–644, 2007.

[7] S.A. Greenhalgh and L. Marescot, "Modeling and migration of 2-D georadar data: a stationary phase approach," *IEEE Trans. Geosci. Remote Sens.*, vol. 44, no. 9, pp. 2421–2429, Sep, 2006.

[8] M. Converse, E.J. Bond, B.D. Van Veen and S.C. Hagness, "A computational study of ultra-wideband versus narrowband microwave hyperthermia for breast cancer treatment," *IEEE Trans. Microw. Theory and Tech.*, vol. 54, no. 5, pp. 2169–2180, May, 2006.

[9] S. Kidera, T. Sakamoto and T. Sato, "A Robust and Fast Imaging Algorithm with an Envelope of Circles for UWB Pulse Radars", *IEICE Trans. Commun.*, vol.E90-B, no.7, pp. 1801–1809, July, 2007.

[10] S. Kidera, T. Sakamoto and T. Sato, "A Robust and Fast 3-D Imaging Algorithm without Derivative Operations for UWB Pulse Radars," URSI. International Symposium on Electromagnetic Theory (EMTS) 2007, Jul. 2007.

[11] S. Kidera, T. Sakamoto, T. Sato and S. Sugino, "An Accurate Imaging Algorithm with Scattered Waveform Estimation for UWB Pulse Radars", *IEICE Trans. Commun.*, vol. E89-B, no. 9, pp. 2588-2595, Sept., 2006

[12] S. Kidera, T. Sakamoto and T. Sato, "A High-Resolution Imaging Algorithm without Derivatives Based on Waveform Estimation for UWB Radars", *IEICE Trans. Commun.*, vol.E90-B, no.6, pp. 1487–1494, June, 2007.

[13] K. Nishimura, T. Sato, T. Nakamura, and M. Ueda, "High Sensitivity Radar-Optical Observations of Faint Meteors," *IEICE Trans. Commun.*, vol.E84-C, no.12, pp. 1877–1884, Dec., 2001.